CHIN.PHYS.LETT. Vol. 25, No. 4 (2008) 1347

Experimental Study on Liquid Free Surface in Buoyant-Thermocapillary Convection *

DUAN Li(段俐), KANG Qi(康琦)**, HU Wen-Rui(胡文瑞)

National Microgravity Laboratory (CAS), Institute of Mechanics, Chinese Academy of Sciences, Beijing 100080

(Received 29 November 2007)

We investigate the surface deformations of buoyant-thermocapillary convection in a rectangular cavity due to gravity and temperature gradient between the two sidewalls. The cavity is 52 mm×42 mm in horizontal cross section, the thickness of liquid layer h is changed from 2.5 mm to 6.5 mm. Surface deformations of h = 3.5 mm and 6.0 mm are discussed and compared. Temperature difference is increased gradually, and the flow in the liquid layer will change from stable convection to unstable convection. Two kinds of optical diagnostic system with image processor are developed for study of the kinetics of buoyant-thermocapillary convection, they give out the information of liquid free surface. The quantitative results are calculated by Fourier transform and correlation analysis, respectively. With the increasing temperature gradient, surface deformations calculated are more declining. It is interesting phenomenon that the inclining directions of the convections in thin and thick liquid layers are different. For a thin layer, the convection is mainly controlled by thermocapillary effect. However, for a thick layer, the convection is mainly controlled by buoyancy effect. The surface deformation theoretically analysed is consistent with our experimental results. The present experiment proves that surface deformation is related to temperature gradient and thickness of the liquid layer. In other words, surface deformation lies on capillary convection and buoyancy convection.

PACS: 47. 20. Bp, 47. 20. Dr, 47. 27. Nd

Thermocapillary convection is driven by the non-uniformity of surface tension, which comes from the non-uniformity of surface temperature.[1] Buoyancy convection is driven by concentration gradient or temperature gradient in gravity. Exploring this convection phenomenon is available in controlling growth of many materials, and obtaining the advanced materials.[2] In ground experiments of thermocapillary convection, gravity influence can not be neglected, since the buoyancy forces are still present. The flow is the coupling of thermocapillary convection and buoyancy convection. It is generally named as buoyant-thermocapillary convection.

The convection brings on surface flow of fluid, and forms a return-flow because of mass conservation. In mechanical theories, there is a shear flow near free surface, which is easy to cause instability or oscillation. When thermocapillary convection or buoyancy convection occurs, surface deformation appears. It is important to research the phenomena for understanding the mechanism of fluid convection. Sen and Davis proved that pressure gradient is directed from the hot side towards the cold side, hence the pressure is higher at the cold side, and the interface bulges near the cold side and is constricted near the hot side.[3] Shu *et al.*[4] studied the influence of free-surface deformation of a liquid bridge by optical diagnostics. Ezersky[5] observed an unstable flow's free surface using shadowgraphic image, and detected the presence of flow-induced surface wave. Previously we systemically measured the surface deformation and surface oscillation of buoyant thermocapillary convection in a cavity, and studied their physical characteristics.[6,7] Dabiri and Gharib[8] measured free surface deformation caused by near-surface turbulence, and it was concluded that energy could be stored in surface deformation during the relaxation of deformation. The techniques of measuring large-deformation have been advanced. Leneweit *et al.*,[9] Lapham *et al.*[10] and Saylor *et al.*[11] used the optical technique to measure fluid surface deformation in millimetre order of magnitude. However, measuring deformation in micron order is very difficult.

In the present experiments, surface deformation is measured by interference method, which is real time and accurate. However, this method can only measure the deformation at the centre of the cavity. Thus, a new optical diagnostic system with image processor has been developed. This system is made up of optical bar lines. Compared with the Michelson interferometer method, this new one gives out the displacement of free surface information at both the centre region and the fringe.

The thermocapillary convection in a cavity is considered, with length a and height h, it is the same as our experiment model. The coordinate system (x, y, z) is used, where $-a/2 \leq x \leq a/2$, the liquid free surface is described by $z = h(x)$, and $\partial/\partial y = 0$. The low temperature is $T_c = T_0$ on the side of $x = -a/2$, and the high temperature is $T_h = T_0 + \Delta T$ on the side of $x = a/2$, as shown in Fig. 1. The basic equations are as follows:

---

*Supported by the National Natural Science Foundation of China under Grant Nos 10672171 and 10432060.

**Email: kq@imech.ac.cn

$$\frac{\partial u}{\partial x}+\frac{\partial w}{\partial z}=0, \tag{1}$$

$$\frac{\partial u}{\partial t}+u\frac{\partial u}{\partial x}+w\frac{\partial u}{\partial z}=-\frac{1}{\rho}\frac{\partial p}{\partial x}+\nu\nabla^2 u, \tag{2}$$

$$\frac{\partial w}{\partial t}+u\frac{\partial w}{\partial x}+w\frac{\partial w}{\partial z}=-\frac{1}{\rho}\frac{\partial p}{\partial z}+\nu\nabla^2 w, \tag{3}$$

$$\frac{\partial T}{\partial t}+u\frac{\partial T}{\partial x}+w\frac{\partial T}{\partial z}=\kappa\nabla^2 T. \tag{4}$$

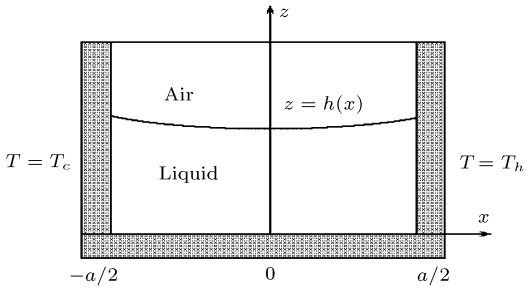

Fig. 1. Thermocapillary convection in a cavity.

The theoretical analyses show that the thermocapillary convection driven by surface tension moves to the cold side near free surface, with the cold side higher than the hot side. The analysed solution is the same as the experimental result on the thermocapillary convection.[2,3]

In the present research, the buoyant-thermocapillary convection consists of a rectangle cavity as shown in Fig. 2. The horizontal cross section of the cavity is 52 mm×42 mm. There is a silicon oil layer in the experimental cavity. The two opposite lateral walls are made of transparent K9 glass for flow visualization. Other two opposite lateral walls are made of copperplates. One of the copperplates is heated by an electro-thermal film, and other one is cooled by semiconductor cooling sheet and a radiator. Temperature difference between the two copperplates in the liquid layer will be formed, which will be measured by thermocouple, and the hot side is controlled by a dc power source. In the present experiment, temperature difference is increased gradually, and the flow in the liquid layer will develop from stable convection to unstable convection.

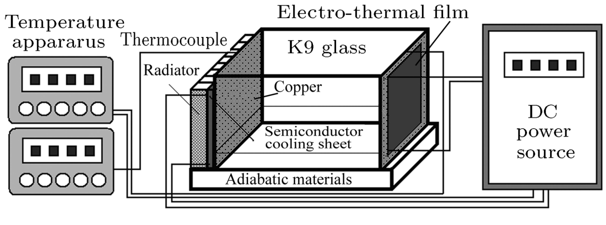

Fig. 2. The controlling system of the convection.

The Michelson interference method is used to measure the free surface deformation of fluid in microns order. The diagram of the optical diagnostic system is shown in Fig. 3. A He–Ne laser beam passes through lenses L1 and L2 to form an expanded parallel light beam, and then the beam is split by a beam splitter BS into two parallel light beams. One is used as the object beam, and the other is used as the reference beam. The object light beam illuminates the liquid surface, and is reflected from the surface, then is reflected again by the beam splitter BS. The reference light beam is reflected by mirror M4, and then passes through the beam splitter BS. At this time, the object beam and the reference beam meet together and form an interferometric fringe pattern on the ground glass D. The fringes carry information of surface deformation caused by convection. The area measured by the interferometer is 18 mm×14.4 mm at the centre of the cavity for the reason of horizontal liquid surface. The image system is composed of a CCD camera and a Pinnacle image system.

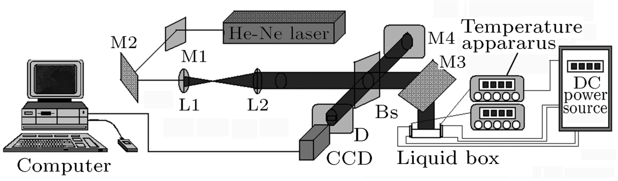

Fig. 3. Optical interference system.

In order to calculate surface deformation from interference fringes, grating analysis with the help of Fourier transform is used. The fringe image at temperature difference 0°C is used as the original grating, and the fringe image at another state is used as the metamorphic grating. First, the phase distributions ϕ_2 and ϕ_1 of the metamorphic grating and the original grating are obtained by Fourier transformation of their fringe images, respectively. Thus, we can work out the phase difference $\Delta\phi=\phi_2-\phi_1$. Finally, the vertical surface deformation of fluid surface $\Delta Z(x,y)$ can be written as

$$\Delta Z(x,y)=\frac{1}{2n}\times\Delta\phi(x,y)\times\frac{\lambda}{2\pi}, \tag{5}$$

where n is the refractive index of air.

The surface deformations for different thicknesses of the liquid layer, i.e. h = 3.0, 3.5, 4.0, 4.5, 5.0, 5.5, 6.0, 6.5 mm, have been measured, and the surface deformations for h = 3.5 mm and h = 6.0 mm are shown and compared. The temperature difference between the two sides of the cavity is increased from 0°C to 58.5°C at the rate of 0.73°C/min. The interference fringes at temperature difference of 0°C is modulated to be horizontal, which is used as the original fringe for the image calculation. The metamorphic fringes due to the deformation of liquid free surface have been captured.

Figure 4 shows the interference fringes at temperature difference of 39.0°C for the layer h = 3.5 mm and h = 6.0 mm. The bent fringes show that the liquid surface deformation for $h = 3.5\,\text{mm}$ and $h = 6.0\,\text{mm}$ are reversed. The changes of deformation are from several microns to 40 microns, as shown in Fig. 5. In the figures, the x-axis is taken in the direction of the temperature gradient of fluid surface, and the Z axis is in the direction upward and vertical to level. The coordinate origin is at the centre of fluid surface. Surface deformations of fluid are correlative directly with temperature gradient, as shown in Fig. 6, which is the deformation in the central line of the liquid layer.

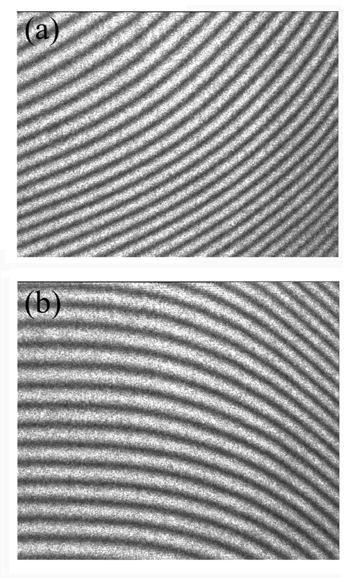

Fig. 4. Interference fringe images at temperature difference of 39.0°C : (a) $h = 3.5\,\text{mm}$, (b) $h = 6.0\,\text{mm}$.

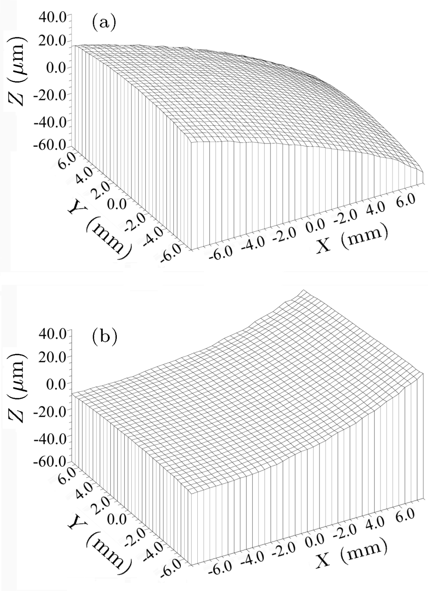

Fig. 5. Surface deformation at temperature difference 39.0°C: (a) $h = 3.5\,\text{mm}$, (b) $h = 6.0\,\text{mm}$.

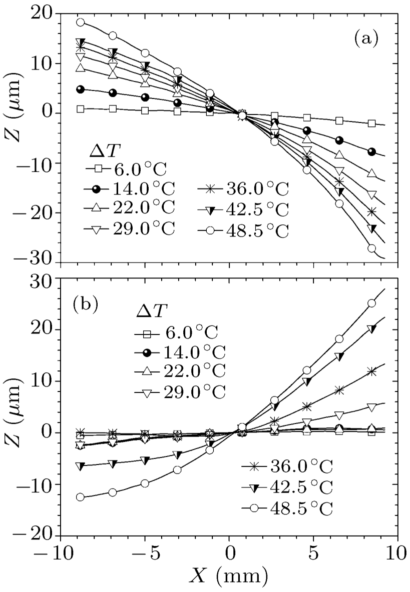

Fig. 6. Surface deformation in the central line of liquid layer: (a) $h = 3.5\,\text{mm}$, (b) $h = 6.0\,\text{mm}$.

Using the interference method, we can only measure the central area of the cavity. In order to avoid the limitation of the interference method, we design optical bar lines to enlarge the measured area, as shown in Fig. 7. A He-Ne laser beam passes through the Wollaston prism, wave slice, polarimeter and forms a baroque light with the bar lines. This baroque light passes through the assembling lens, and focuses on the liquid surface, and then reflects and comes to the ground glass. The bar lines carry the information of surface deformation caused by capillary convection and/or buoyancy convection. The image system is composed of a CCD camera and a Superdv image system.

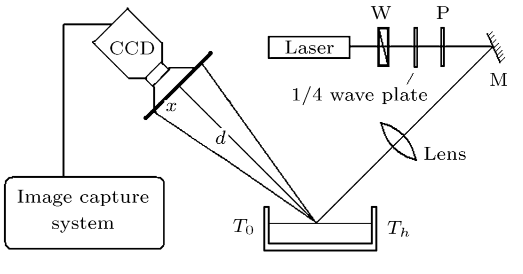

Fig. 7. Optical diagnostic system.

We use correlation analysis to calculate the surface deformation from bar line images. The image at 0°C temperature difference is taken as the original one, it gives out matrix $A(m,n)$, $0 \le m \le M_a - 1$, $0 \le n \le N_a - 1$, $M_a = 576$, $N_a = 720$. First, the deformation is zero, then the video is translated into images (25 frames/s), the images are gained (at the temperature differences of 10, 20, 30, 40, 50°C), if $B(m,n)$ is the matrix at temperature difference 10°C, then $\rho(i,j)$ is the standard correlation function of A and B. Here i and j are the relatively pixel displacement when the dimensionless $\rho(i,j)$ gets to the maximum; m, n, i, j, M_a, and N_a are in units of pixel. Then we can reach the bar line excursion

$$X = i/54. \tag{6}$$

For the numeration of $\rho(i,j)$,

$$C(i,j) = \sum_{m=0}^{M_a-1}\sum_{n=0}^{N_a-1} A(m,n)\text{conj}[B(m+i,n+j)], \tag{7}$$

$$0 \le i < M_a + M_b - 1, \quad \text{and} \quad 0 \le j < N_a + N_b - 1,$$
$$M_a = 576, \quad N_a = 720, \tag{8}$$

$$\rho(i,j) = C(i,j)\Big[\sum\nolimits_{m=0}^{M_a-1}\sum\nolimits_{n=0}^{N_a-1} A^2(m,n) \cdot \sum\nolimits_{i=0}^{M_a-1}\sum\nolimits_{j=0}^{N_a-1} B^2(m+i,n+j)\Big]^{-1/2}. \tag{9}$$

The bar line excursion is x, the distance between the ground glass and liquid surface is $d = 270\,\text{mm}$, x and d are labelled in Fig. 7. The excursion angle of the lines is $\alpha = \arctan(x/d)$, surface excursion angle is $\beta = 0.5\alpha$. The slope alteration is $\Delta k = \tan(\beta)$; k is the slope of the surface at temperature difference of zero, so we obtain the last slope $K = k - \Delta k$. Now we can reach the curve of the liquid surface by integral formula. On the assumption that volume of the liquid is changeless, we can confirm the zero point. Then the height of liquid surface is confirmed.

In the present experiment, surface deformations of silicon oil layers in different thicknesses ($h = 3.5$ mm, 6.0 mm) have been observed separately. Temperature difference between the two sides of the cavity is increased from 0°C to 50°C at the rate of 0.6°C/min. The bar line at temperature difference of 0°C is modulated to be horizontal, as shown in Fig. 8(a) ($h = 3.5$ mm), which is taken as the original fringe for the image calculation. The metamorphic fringes which stand for the deformation of liquid free surface have been captured. The fringes move to a certain direction, and the liquid surface is more slanting with the increasing temperature gradient. Figure 8(b) shows the fringes at the temperature difference of 10°C ($h = 3.5$ mm). Figure 9 shows the correlation of Figs. 8(a) and 8(b).

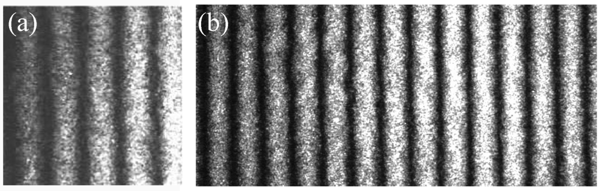

Fig. 8. The bar line image at different temperature differences: (a) the bar lines at $\Delta T = 0$°C (200 × 200 pixel), (b) bar lines at $\Delta T = 10$°C (250 × 550 pixel).

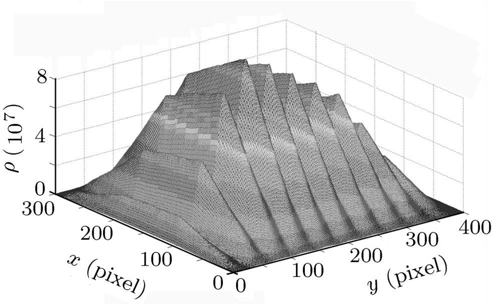

Fig. 9. Correlation of the images.

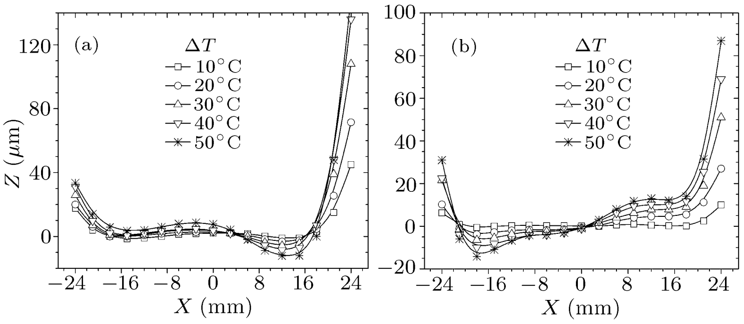

Fig. 10. Deformation on central line for different thicknesses of the layer by optical bar line method: (a) 3.5 mm, (b) 6 mm.

Figure 10 shows the deformation on central lines of the cavity for different heights ($h = 3.5$ mm and $h = 6$ mm) of layer by optical bar line method, which is also coincident with the result measured by the interference method.

The optical bar line experiment gives out the surface deformation at the area of $-25 < x < 25$, which is almost the entire region of the liquid surface. The two experiments by the optical bar lines method and the interference method give out the same trend of surface deformation at the centre of the container. In the results of interference method, the deformation curve is monotone ($-9\,\text{mm} < x < 9\,\text{mm}$), and there is a peak value in the results of the optical bar line method. This is induced by many reasons, such as the difference of temperature gradient. The experiments demonstrate the function of the capillary and buoyancy. For the thin layer, the gradient of surface tension mainly controls the convection, the cold side is higher than the hot side because of liquid moving from the hot side to the cold side with increasing temperature difference. For the thick layer, buoyancy mainly controls the convection, the hot side is higher than the cold side because of the effect of buoyancy convection.

In addition, it can be found from the second experiment that the liquid climbs up the sidewalls of the cavity, which is the soakage phenomenon between solids and liquids. The thicknesses of the layers in both sides become higher with the increasing temperature, as shown in Fig. 10, which is well regulated.

In summary, we have used the interference technique and bar line technique to measure the free surface of fluid, and obtained the quantitative results. Surface deformation of buoyant-thermocapillary convection has been measured. With the increasing temperature gradient, the liquid surface slants gradually. The surface inclining directions of convections in thin and thick liquid layers are different, which expresses the different functions of thermocapillary effect and buoyancy effect. In addition, the soakage phenomenon between solids and liquids influences the liquid free surface.

References

[1] Burguete J et al 2001 *Phys. of Fluids* **13** 2773
[2] Schatz M F et al 2001 *Ann. Rev. Fluid Mech.* **33** 93
[3] Sen A K and Davis S H 1982 *J. Fluid Mech.* **121** 163
[4] Shu J Z et al 1994 *Microgravity Sci. Technol.* **7** 83
[5] Ezersky A B et al 1993 *Phys. Rev.* E **47** 1126
[6] Duan L, Kang Q and Hu W R 2006 *Sci. Chin.* E **49** 601
[7] Kang Q, Duan L and Hu W R 2004 *Microgravity Sci. Technol.* **XV** 18
[8] Dabiri D and Gharib M 2001 *Exp. Fluids* **30** 381
[9] Leneweit G et al 1999 *Exp. Fluids* **26** 75
[10] Lapham G S et al 2001 *Exp. Fluids* **30** 448
[11] Saylor J R et al 2000 *Exp. Fluids* **29** 509